# Reaction-diffusion waves in hydro-mechanically coupled porous solids as a precursor to instabilities

**Qingpei Sun[1], Manman Hu[1], Christoph Schrank[2], Klaus Regenauer-Lieb[3]**

[1]Department of Civil Engineering, The University of Hong Kong, Hong Kong

[2]School of Earth and Atmospheric Sciences, Queensland University of Technology, Brisbane, QLD, Australia

[3]School of Minerals and Energy Resources Engineering, UNSW, Sydney, NSW, Australia

**Key Points:**

- A new class of nonlocal reaction-diffusion equations models Earth instabilities
- Stationary and travelling dissipative waves are predicted
- Turing, Hopf and quasi-soliton waves create barcode-like fault damage zones

Corresponding author: Manman Hu, mmhu@hku.hk

**Abstract**

Here, we extend the Fisher-Kolmogorov-Petrovsky-Piskunov equation to capture the interplay of multiscale and multiphysics coupled processes. We use a minimum of two coupled reaction-diffusion equations with additional nonlocal terms that describe the coupling between scales through mutual cross-diffusivities and regularise the ill-posed reaction-self-diffusion system. Applying bifurcation theory we suggest that geological patterns can be interpreted as physical representations of two classes of well-known instabilities: Turing instability, Hopf bifurcation, and a new class of complex soliton-like waves. The new class appears for small fluid release reactions rates which may, for negligible self-diffusion, lead to an extreme focusing of wave intensity into a short sharp earthquake-like event. We propose a first step approach for detection of these dissipative waves, expected to precede a large scale instability.

## Plain Language Summary

Regular and irregular patterns of deformation bands and fractures are ubiquitous in nature. In this paper, we decipher the patterns in terms of coefficients of a simple set of reaction-diffusion equations that can, for given material parameters, describe a transition from regular to logarithmically decaying patterns and chaotic instabilities. Similar sets of equations have previously been used to explain phenomena in complex chemistry and pattern formation in epidemiology, but without the multiscale and multiphysics consideration for saturated porous media presented here. This work introduces the mathematical formulation and analysis. Quantitative applications to geological observation will follow. The new dissipative waves discovered in this contribution opens an avenue for earthquake forecasting as under extreme conditions they can focus wave energy from the environment into a high intensity localised wave. Immediately before the main event occurs there is a reduction of background wave amplitude to feed the sharp instability. The typical self-focusing wave shape and the 'calm before the storm' is suggested to be tested as a diagnostic forecasting tool of earthquakes.

## 1 Introduction

Travelling-wave solutions of reaction-diffusion systems are encountered in many fields, e.g. in chemistry, epidemiology, biology, medicine, and physics. They were first identified in chemistry by R. Luther in 1906 and demonstrated in an experiment where oxalic acid mixed with potassium permanganate led to a wave propagation of the reaction made visible by an oscillatory front of decolorization of the mixture. An English translation of the transcript of the original lecture has been published much later (Luther, 1987). Subsequently, the same fundamental partial differential reaction-diffusion equation was shown by R.A. Fisher to explain wave-like propagation of mutant genes (Fisher, 1937), which is widely used in epidemiology for modeling the spread of viruses as well as in many other fields of biology (Volpert & Petrovskii, 2009). The equation is now better known as the Fisher-Kolmogorov-Petrovsky-Piskunov (FKPP) equation (Kolmogorov et al., 1937), recognizing the important early work (Adomian, 1995).

Although the basic mathematical equation is agnostic of the application, and the phenomenon is now well established in the above named disciplines, it has found little application in the Earth Science field so far, where reaction-diffusion problems are common. Pioneering work was presented in the 1990's (Dewers & Ortoleva, 1990; Ortoleva, 1993, 1994). Not much progress has been made on further development of geophysical applications to the slow travelling-wave solution. Broader community interest was mainly met for the special case of the stationary solution of the system of equations (Ball, 2012). The main problem in the application to Earth Sciences is perhaps twofold. The first problem is that patterns in nature are mostly observed as frozen in features of the dynamic solution. It is difficult to discern from geological observations, whether the rhythmic fea-

tures are frozen-in patterns of an oscillating reaction-diffusion equation propagating in time (Hopf-bifurcations), or whether they are caused by a standing wave solution (Turing-patterns) fixed in space (L'Heureux, 2013). The second problem is that the original FKPP equation does not replicate the rich field of observations encountered in nature.

For geological applications, a generalized power-law reactive source term therefore has been proposed as an extension to the FKPP equation (Vardoulakis & Sulem, 1995). Using the simple case of a time-independent reaction-diffusion equation with a power-law reactive source term and integer-valued exponents, standing solitary wave Korteweg-De Vries (KdV)-type solutions were obtained analytically (Regenauer-Lieb et al., 2013; Veveakis & Regenauer-Lieb, 2015). The inclusion of the power-law source term unfortunately leads to an infinite amplitude KdV-type solitary wave. Several attempts have been made to overcome this shortcoming with the aim to provide an appropriate application for modelling compaction bands in porous (or multiphase) geomaterials. One solution proposes, for instance, an additional reaction source term buffering the instabilities for carefully chosen cases (Alevizos et al., 2017). While the proposed approaches manage to achieve a solution to the ill-posed problem of lacking an internal material length for some cases, a generalized approach is in absence.

Here, we develop a theory that has the potential to solve the problem directly for all cases by using an approach that is based on internal length scales stemming from the physics of the feedbacks of multiple processes operating across multiple characteristic scales. We introduce the lacking internal material length scale through an integration of non-local diffusion and reaction coefficients originating from lower-scale processes. In a simple formulation, the feedbacks can be captured mathematically by the interaction between at least two reaction-diffusion equations coupled through two sufficiently large cross-diffusion coefficients between interweaved dynamic systems, e.g., a saturated porous medium in the post-yield regime (Hu et al., 2020).

The system of equations has been generalized to describe multiphysics couplings between multiple scales (Regenauer-Lieb et al., 2021b). In such a formulation, the cross-diffusion coefficients are derived through volume integration of diffusion processes that are spatially connected to interactions at the lower scale and therefore also called non-local diffusion processes. In this sense, the diffusion of a given concentration of species does not only depend on its position in space and its gradient, but also on the nonlocal effect of the values of concentrations around it and the convolution of the concentration with the probability distribution to jump from one location to another (Amdreo-Valle et al., 2010). Such nonlocal diffusion processes have recently attracted much attention in the mathematics community as the FKPP-equation was found to display unexpected wave front accelerations due to the nonlocal terms, as first observed in the invasion of cane toads in Australia (Bouin et al., 2017).

As an innovation in this paper, we also consider nonlocal reactions where the non-locality arises from modeling the behavior of one phase interacting with another in its immediate environment and vice versa, concurrently - lending itself to a dynamical system approach that captures the multiphysics involved in a tightly coupled fashion. The beauty of this new class of nonlocal approaches lies in the fact that it naturally allows process coupling across spatial and temporal scales where runaway reactions can be buffered via infinite-speed propagation of such perturbations through the nonlocal diffusion process (Amdreo-Valle et al., 2010). In the Supporting Information we perform a linear stability analysis of the newly proposed system of equations and provide a systematic analysis of the parametric space. In the following we summarize the basic formulation and its three fundamentally different types of instabilities and discuss possible applications in geology and geophysics.

## 2 Korteweg-De Vries-type standing-wave limit

The dynamic equation for the momentum balance of the solid skeleton in a hydro-poromechanic nonlinear visco-plastic medium is expressed in the Perzyna overstress (Duszek-Perzyna & Perzyna, 1996) formulation (describing the viscous material behaviour post yield) as a FKPP-type reaction-diffusion equation:

$$\frac{\partial \bar{p}_s}{\partial t} = D_M \frac{\partial^2 \bar{p}_s}{\partial x^2} + R_1, \tag{1}$$

where in the above 1-D formulation $\bar{p}_s$ denotes the Perzyna overpressure for the solid skeleton and $R_1$ a nonlinear reactive source pressure term.

Under the standing-wave assumption, this travelling-wave equation becomes a static mechanical viscous overpressure reaction-diffusion equation:

$$D_M \frac{\partial^2 \bar{p}_s}{\partial x^2} + R_1 = 0. \tag{2}$$

The coupled dynamic fluid pressure system can be described by a similar wave equation:

$$\frac{\partial p_f}{\partial t} = D_H \frac{\partial^2 p_f}{\partial x^2} + R_2, \tag{3}$$

which for the static case with a zero source term $R_2$ becomes the Darcy equation:

$$D_H \frac{\partial^2 p_f}{\partial x^2} = 0. \tag{4}$$

We introduce a dimensionless form

$$\tilde{p}_s = \frac{\bar{p}_s}{p'_{ref}}\ ,\ \tilde{x} = \frac{x}{l_0}, \lambda = \frac{D_M}{D_H}, \tag{5}$$

where $p'_{ref}$ and $l_0$ are reference pressure and reference length, respectively. Assuming a power-law reactive pressure source term with a power-law exponent $m$, the coupled system of equations (2) and (4) becomes a Korteweg-De Vries-type standing wave equation:

$$\frac{\partial^2 \tilde{p}_s}{\partial \tilde{x}^2} - \lambda \tilde{p}_s^m = 0. \tag{6}$$

Analytical solutions for the practical application to compaction bands with $m = 3$ have been suggested (Regenauer-Lieb et al., 2013; Veveakis & Regenauer-Lieb, 2015), which feature, for a critical ratio of solid/fluid self-diffusivities $\lambda > 12.7$, periodic standing waves with infinite-amplitude singularities of the non-dimensional overpressure.

## 3 Cross-diffusion equations in geomaterials

The system of equations can be regularized by extending equations (1) and (3) through nonlocal cross-coupling diffusivities between the two dynamic systems considering the unique structure of porous media (Hu et al., 2020). Such cross-couplings are well known in chemistry as cross-diffusion (Vanag & Epstein, 2009) between chemically reactive constituents. In our case, cross-diffusion arises as interfacial characteristics (Hu et al., 2020) and regularizes the feedbacks between the dynamic evolution of the fluid and solid pressure. The equations for a fully saturated porous medium post yield can be expressed as:

$$\frac{\partial \bar{p}_s}{\partial t} = D_M \frac{\partial^2 \bar{p}_s}{\partial x^2} + d_H \frac{\partial^2 p_f}{\partial x^2} + R_1, \tag{7}$$

$$\frac{\partial p_f}{\partial t} = d_M \frac{\partial^2 \bar{p}_s}{\partial x^2} + D_H \frac{\partial^2 p_f}{\partial x^2} + R_2, \tag{8}$$

where $R_1$ and $R_2$ are the reaction terms in the governing equations for solid and fluid pressure, respectively. For completeness, we extend the formulation of the crossover diffusion problem proposed earlier (Hu et al., 2020) by nonlocal reaction terms. This allows us to explore a more general solution space.

For expanding the reaction term $R_2$ in Eq.(8), we need to consider the feedback between solid and fluid pressure reactions. The reaction term $R_2$ incorporates cross-scale coupling to gradients of the pressure in the solid matrix $p_s$ in the surrounding pore space, which exerts a "nonlocal" effect on the fluid pressure $p_f$ inside the pore. For the local source term, we assume a simple linear process for the fluid phase, which can be water production/depletion due to dehydration/rehydration of minerals. Thus, to take into account the above two factors, we assume that the reaction term $R_2$ follows a linear function of the fluid pressure and solid overstress, i.e. $R_2 = a_{21}\bar{p}_s + a_{22}p_f$, where $a_{21}$ and $a_{22}$ are the corresponding coefficients.

Likewise, the reaction term $R_1$ in Eq.(7) is translated into a nonlocal reaction formulation as we expand the power-law assumption in (Veveakis & Regenauer-Lieb, 2015) by higher order terms of $\bar{p}_s$ to describe the viscoplastic behaviour of the solid skeleton. The feedback to the fluid pressure $p_f$ is, however, assumed to be linear, for simplicity. The generalized reaction term in Eq.(7) is now written in a non-linear form of $R_1 = a_{11}\bar{p}_s + a_{12}p_f + a_{13}\bar{p}_s^2 + a_{14}\bar{p}_s^3$. Note that all the coefficients in the reaction terms would also evolve according to the in-situ chemo-hydro-mechanical conditions, but here we just give the generalized form and regard them as constants to facilitate the analysis.

By introducing the dimensionless parameters $\tilde{t} = \dot{\varepsilon}_0 t$, $\tilde{p}_f = \bar{p}_f / p'_{ref}$, where $\dot{\varepsilon}_0$ denotes the reference strain rate, together with the previously defined $\tilde{p}_s = \frac{\bar{p}_s}{p'_{ref}}$ ,$\tilde{x} = \frac{x}{l_0}$, we arrive at the normalized cross-diffusion equations with normalized reaction terms $\tilde{R}_1$ and $\tilde{R}_2$ expressed as

$$\frac{\partial \tilde{p}_s}{\partial \tilde{t}} = \tilde{D}_M \frac{\partial^2 \tilde{p}_s}{\partial \tilde{x}^2} + \tilde{d}_H \frac{\partial^2 \tilde{p}_f}{\partial \tilde{x}^2} + \tilde{a}_{11}\tilde{p}_s + \tilde{a}_{12}\tilde{p}_f + \tilde{a}_{13}\tilde{p}_s^2 + \tilde{a}_{14}\tilde{p}_s^3, \tag{9}$$

$$\frac{\partial \tilde{p}_f}{\partial \tilde{t}} = \tilde{d}_M \frac{\partial^2 \tilde{p}_s}{\partial \tilde{x}^2} + \tilde{D}_H \frac{\partial^2 \tilde{p}_f}{\partial \tilde{x}^2} + \tilde{a}_{21}\tilde{p}_s + \tilde{a}_{22}\tilde{p}_f, \tag{10}$$

where $\tilde{D}_M = \frac{D_M}{{l_0}^2 \dot{\varepsilon}_0}$, $\tilde{d}_H = \frac{d_H}{{l_0}^2 \dot{\varepsilon}_0}$, $\tilde{a}_{11} = \frac{a_{11}}{\dot{\varepsilon}_0}$, $\tilde{a}_{12} = \frac{a_{12}}{\dot{\varepsilon}_0}$, $\tilde{a}_{13} = \frac{a_{12}p'_{ref}}{\dot{\varepsilon}_0}$, $\tilde{a}_{14} = \frac{a_{12}{p'_{ref}}^2}{\dot{\varepsilon}_0}$, $\tilde{d}_M = \frac{d_M}{{l_0}^2 \dot{\varepsilon}_0}$, $\tilde{D}_H = \frac{D_H}{{l_0}^2 \dot{\varepsilon}_0}$, $\tilde{a}_{21} = \frac{a_{21}}{\dot{\varepsilon}_0}$, $\tilde{a}_{22} = \frac{a_{22}}{\dot{\varepsilon}_0}$.

In this paper, we describe only two coupled nonlocal reaction-diffusion processes. It is straightforward to extend the approach into a higher degree of coupling such as an interaction with a thermal nonlocal reaction diffusion equation. Without loss of generality, we also limit the higher-order expansion to the order 3 for numerical analysis to capture the essential features of the formulation. In our investigation, an order 3 was the minimum requirement to obtain the full spectrum of solutions including excitation waves. The development of a concise formulation for extension to higher degrees of coupling is never a trivial task considering the complexity associated with new spatial and temporal scales introduced into the system, and is hence out of the scope of this letter. A simplified meso-scale formalism is proposed in (Regenauer-Lieb et al., 2021b) by adding additional cross- and self-diffusion coefficients to the system of equations via the fully populated true diffusion matrix.

### 3.1 System constraints and system behaviour

In what follows, the behaviour of a system of a saturated porous material described by Eq.(9) and Eq.(10) for $\tilde{p}_s : \Omega \to \mathcal{R}^1$ and $\tilde{p}_f : \Omega \to \mathcal{R}^1$, respectively, will be investigated. We use a classical formulation for modelling wave-propagation problems. Non-flux boundary conditions are assumed: $\mathbf{n} \cdot \nabla \tilde{p}_s = 0$ and $\mathbf{n} \cdot \nabla \tilde{p}_f = 0$ for $x \in \partial\Omega$. Here, $\Omega \subset \mathcal{R}^n$ is a smooth bounded domain with outer unit normal $\mathbf{n}$ and total volume $\mid \Omega \mid$. The initial condition is assumed as $\tilde{p}_s(x,0) = \tilde{p}_f(x,0) = 0$ for $x \in \Omega$, for simplicity.

In terms of the Perzyna overstress model used in this formulation, the system size is considered to correspond to the region where the overstress has been reached due to loading from the far field. The non-flux boundary conditions then correspond to the elastic-plastic boundary. In what follows, we arbitrarily choose the left boundary as the one where the system receives a perturbation from the outside which may lead to material failure within or at the boundaries of the system.

While the addition of a cross-diffusion term allows a fast response to the coupling of the two dynamical equations, thus regulating the coupled system by the new cross-diffusivities, the equations become no longer tractable in analytical form. The coupling terms may also give rise to new instabilities, for which the linear stability analysis (see Supporting Information) provides a robust derivation. With sufficiently large perturbation applied on the left boundary of the domain, three different types of instabilities are encountered: (1) Turing instabilities, (2) Hopf-bifurcations, and (3) cross-diffusional waves. The corresponding systems are investigated numerically in the following subsections. Selections of parameters are based on the linear stability analysis presented in the Supporting Information.

### 3.2 Turing bifurcations

When the system undergoes Turing bifurcations, standing waves are generated, leading to space-periodic patterns. Turing bifurcations require the system to be stable when diffusion is not considered, and an unstable saddle comes into effect when the control parameters vary (see Supporting Information). In our formulation, the phase space is spanned by the two main variables $\tilde{p}_s$ and $\tilde{p}_f$, and the main control variables for these are $\tilde{a}_{11}$ snd $\tilde{a}_{22}$, scaling the sign and magnitude of the solid and fluid pressure reactive source terms, respectively. A saddle point in the $\tilde{p}_s$ - $\tilde{p}_f$ phase space is defined as a critical point where the phase switches from a stable manifold to an unstable manifold. In other words: (I) a stable manifold is achieved via $Re(s_k) < 0$, i.e. the real part of $s_k$ being negative, when the wavenumber $k = 0$; (II) an unstable manifold exists with the variation of wavenumber $k$, if a real positive number (no imaginary part) exists for $s_k$, which corresponds to the growth rate of the perturbation. To satisfy the above requirements, a sufficient condition for the onset of Turing instabilities is summarized as follows:

(a) $\mathrm{tr}_0 = \tilde{a}_{11} + \tilde{a}_{22} < 0$, where $\mathrm{tr}_0$ denotes the value of $\mathrm{tr_k}$ for wavenumber $k = 0$.

(b) $\Delta_0 = \tilde{a}_{11}\tilde{a}_{22} - \tilde{a}_{12}\tilde{a}_{21} > 0$, where $\Delta_0$ denotes the value of $\Delta_k$ for wavenumber $k = 0$.

Here, $\mathrm{tr_k}$ and $\Delta_k$ are coefficients in the characteristic polynomial of $s_k$ as defined in the Supporting Information.

(c) At the critical wavenumber $k_c$,

$$k_c^2 = \frac{\tilde{a}_{11}\tilde{D}_H + \tilde{a}_{22}\tilde{D}_M - \tilde{a}_{21}\tilde{d}_H - \tilde{a}_{12}\tilde{d}_M}{2(\tilde{D}_M\tilde{D}_H - \tilde{d}_M\tilde{d}_H)},$$

$$\Delta_{k_c} = \Delta_0 - \frac{(\tilde{a}_{11}\tilde{D}_H + \tilde{a}_{22}\tilde{D}_M - \tilde{a}_{21}\tilde{d}_H - \tilde{a}_{12}\tilde{d}_M)^2}{4(\tilde{D}_M\tilde{D}_H - \tilde{d}_M\tilde{d}_H)} < 0.$$

Since the current cross-diffusion formulation is essentially a mass balance based approach, it is expected that the two self-diffusion coefficients $\tilde{D}_M$ and $\tilde{D}_H$ are positive and that the two cross-diffusion coefficients $\tilde{d}_M$ and $\tilde{d}_H$ are of opposite sign. Hence, $(\tilde{D}_M\tilde{D}_H - \tilde{d}_M\tilde{d}_H) > 0$ is naturally satisfied, i.e. $\Delta_k$ at the critical wavenumber corresponds to a local minimum. This criterion combines the self- and cross-diffusion coefficients and extends the original formulation for Turing instabilities in a hydromechanically coupled 1-D system (Regenauer-Lieb et al., 2013; Veveakis & Regenauer-Lieb, 2015).

It is worth noting that the characteristic Turing wavelength is an intrinsic characteristic for the reaction-diffusion equation. It is $\lambda = 2\pi/k_c$, which shows that the wave length is determined by the material coefficients and the system properties comprising the diffusivities and the size of the system (plastic zone) considered (Regenauer-Lieb et al., 2013). This implies that, if the size of the plastic zone is known, the diffusive material properties can directly be derived from the observation of the localisation pattern, e.g., the spacing of fractures or deformation bands (Elphick et al., 2021; Hu et al., 2020), since the diffusion properties also control the spacing of the pattern.

To illustrate the Turing bifurcation solution, we plot numerical results obtained with the Finite Difference Method (FDM) in Fig. (1a) and Fig. (1b). The Turing-style instabilities lead to an equally spaced segmentation of the plastic zone with a distinct striped pattern of localisation (Fig. 1b). Upon continued deformation, the system size and the diffusivities change because inelastic strain localisation modifies the material properties, strain, and the local state of stress. For example in the case of compaction of the plastic zone, the entire zone shrinks continuously, accommodated by discrete Turing-patterned compaction bands. Compaction also changes the diffusivities because permeability is commonly reduced due to inelastic porosity loss through, e.g., grain crushing in the bands (Elphick et al., 2021). Finally, low-porosity compaction bands are also expected to cause local elastic stress amplification, facilitating further strain localisation (Elphick et al., 2021). These effects are not considered in our current calculation. However, for cases where only small deformations are encountered, we expect preservation of Turing-style deformation since the Turing standing wave is essentially a stationary solution.

### 3.3 Hopf bifurcations

When the system undergoes Hopf bifurcations, travelling waves are generated, and temporally periodic (oscillation) patterns can be found (see Fig. 2). The Hopf bifurcation changes a stable focus ($\mathrm{Re}(s_k) < 0$) into an unstable one ($\mathrm{Re}(s_k) > 0$) with the change of control parameters. This requires the existence of certain complex number $s_k$ with the real part (i.e., $\frac{1}{2}\mathrm{tr}_k$) no less than zero when the wavenumber $k$ varies. Given that the maximum value of $\mathrm{tr}_k$ is always obtained when $k = 0$, the above requirement for Hopf instability can be translated to $\mathrm{tr}_0 = \tilde{a}_{11} + \tilde{a}_{22} \geq 0$, $\mathrm{tr}_0{}^2 - 4\Delta_0 = (\tilde{a}_{11} + \tilde{a}_{22})^2 - 4(\tilde{a}_{11}\tilde{a}_{22} - \tilde{a}_{12}\tilde{a}_{21}) < 0$.

The characteristics of Hopf bifurcations are illustrated with numerical solutions obtained with FDM in Fig. (1c) and Fig. (1d). The periodic solutions are similar to Turing bifurcations, replacing a singular frequency spectrum with an exponentially decaying frequency spectrum (Fig. 1c). The oscillation frequency $f$ of the Hopf bifurcation is an intrinsic material property of the reaction-diffusion equation and is defined by $f = 1/T = \sqrt{\tilde{a}_{11}\tilde{a}_{22} - \tilde{a}_{12}\tilde{a}_{21}}/2\pi$. Inversion of material properties from temporal observation thus appears to be possible.

In our example calculation shown in Fig. (1c) and Fig. (1d), the frequency spectrum has distinct gaps between the longest waves and the shortest wavelength at the zero-flux (reflecting) opposite boundary of the plastic zone. As the waves are dissipative, they act like damage waves that continuously change the mechanical properties of the medium

they traverse. An important observation is that the travelling Hopf wave does not reflect from the system boundary but dumps its energy into the boundary.

### 3.4 Cross-diffusion waves for the excitable system

With the variation of parameters in reaction terms $\tilde{R}_1$ and $\tilde{R}_2$, we encounter a slow reaction case where the coefficients in $\tilde{R}_2$ are much smaller than those in $\tilde{R}_1$. In this case, the whole system would become excitable, and soliton-like behaviours can be observed. This situation differs significantly from the above solutions. Upon initiation, the wave does not contain information of the system size but constitutes a pure material instability, carrying only information on the material defining the cross-diffusion matrix (Tsyganov et al., 2007). Upon reflection on the opposite boundaries of the plastic zone, the wave can, however, 'sense' the system size and alter its behaviour accordingly. A special characteristic of a quasi-soliton is that it does not depend on initial conditions but its propagation velocity is a material constant which does not alter after reflection (Tsyganov et al., 2007).

Fig. (1e) and Fig. (1f) illustrate the behaviour of quasi-soliton travelling waves in an excitable system prior to collision or reflection on boundaries with numerical simulations. Our results show that the frequency content changes after interaction with boundaries. Fig. (1e) shows the frequency spectrum after first collision with the boundary where the wave picks up its first information of the system size. Prior to collision with the right boundary, the wave is unaffected by the system size, which is an important difference to the Turing- and Hopf-style instability. The speed of the dominant wave group of the quasisoliton is a material property and independent of initial conditions (Tsyganov et al., 2007). An important aspect is the maximum amplitude at zero frequency, or 'infinite' wavelength, which suggests that relativistic considerations may need to be introduced for high wave speeds which are not expected to be encountered in geological applications. In our case the speed of the wave is limited by the Hadamard jump condition (Regenauer-Lieb et al., 2021b). We show in Fig (1e) a frequency plot after interaction with the opposite boundary which moves the zero frequency maximum to a low frequency maximum.

The frequency spectrum and the behaviour of these waves are complex. Our numerical results show that the cross-diffusion waves can behave like solitons, i.e., they can penetrate through each other or reflect from boundaries. However, there are a number of significant differences (Tsyganov & Biktashev, 2014): (1) their amplitude and speed depend entirely on material parameters whereas those of true solitons depend on initial conditions, (2) true solitons do not change after interpenetration or reflection from boundaries while quasi-soliton waves change frequency spectrum and amplitudes after interaction, and (3) their peculiar behaviour upon collision/reflection classifies them as quasi-solitons encountered in particle physics as they behave like unstable particles (Lioubashevski et al., 1996) and in the extreme case can lead to catastrophic instabilities (Eberhard et al., 2017) sampling wave energy over multiple length scales to release it as a damaging rogue wave.

## 4 Discussion

Turing and Hopf-bifurcations are well-known in geological applications particularly as interpretations of patterns in deformed metamorphic rocks (Hobbs et al., 2011; Hobbs & Ord, 2015; L'Heureux, 2013, 2018). Turing patterns as dissipative structures of reaction-diffusion systems have been claimed to underpin the common principles for the universality of certain basic forms encountered in nature such as hexagons, stripes, fractal shapes and spirals (Ball, 2012). Accordingly, Hopf- and Turing bifurcations are postulated to be encountered in many guises in material- and geoscience applications. Propagating zones of localised deformation have been encountered in metals, polymers and rocks. In the

latter application they are known as 'deformation bands' (Aydin & Johnson, 1978). The similarity of wave-like deformation bands in material science and multiscale patterns in fault damage zones has been highlighted (Makarov & Peryshkin, 2017). It is therefore an attractive proposition to quantify fundamental pattern forming processes in terms of dynamic coefficients of simple reaction-diffusion equations and establish a material database of these coefficients for detection and prediction of material and chemical instabilities that cause emergence of these patterns.

There exists, however, to date no commonly accepted technique to derive the necessary dynamic coefficients as material parameters that control dynamic and static evolution of these patterns. While Hopf- and Turing patterns appear to be frequently encountered in nature the simple reaction-diffusion equation may just not explain the rich solution space. Some elementary ingredient may be missing. We have pointed out that known analytical and numerical solutions to the reaction-diffusion equations often do not converge to physical meaningful solutions as they generally lack an internal length scale that controls the width of pattern forming processes. A good illustration for this is the analytical solution of a simple reaction-diffusion equation (equation 6) with a power law reaction term which has been used for the interpretation of Turing-style instabilities in compacted rocks (Regenauer-Lieb et al., 2013; Veveakis & Regenauer-Lieb, 2015). The solution predicts an infinite wave amplitude on the wave crest singularities. We have therefore proposed that the missing ingredient is indeed the cross-diffusion term which controls the width of instabilities and reduces runaway reactions on wave crests to finite amplitude instabilities (Hu et al., 2020; Regenauer-Lieb et al., 2021a).

Our approach provides a simple and concise mathematical formula to capture the above-described natural phenomena in geology and geophysics. It has been proposed as a system of equations with the lowest degrees of freedom to describe the many intriguing features of reaction-diffusion systems. This approach offers a reaction-diffusion-based process interpretation of patterns observed in nature. The new equations encapsulate an internal material length scale providing a generic regularisation of boundless amplitudes of instabilities for all reaction-diffusion cases considered. This avoids the design of specialised solutions with carefully chosen added reaction or self-diffusion terms as discussed in the introduction. However, they are not merely mathematically convenient for stabilising numerical modelling and interpretation of patterns in nature but they open a new avenue for forecasting instabilities as they propose a new class of waves which provide a testable prediction for the validity of the approach. Moreover, these quasi-soliton (cross-diffusion) waves are expected to precede and lead to the formation of Hopf- and Turing instabilities as shown in the parametric study provided in the Supporting Information. We propose that they constitute the missing physics for the emergence of these instabilities. The new class of waves only occur in excitable systems when sufficiently large fluxes of cross diffusion are encountered (Tsyganov et al., 2007).

The relationship between the three types of instabilities is argued to be of evolutionary type. A material point should change properties after the propagation of a cross-diffusion wave, and the geological structures formed by either Hopf- or Turing style instabilities are generating internal material interfaces. Therefore, while we predict (see the parametric space in the Supporting Information) strictly defined interfaces between the three types of instabilities, in reality evolutionary crossovers between the instability regimes are expected from cross-diffusion waves to Hopf- or Turing instabilities because the material properties evolve dissipatively. Obviously, natural phenomena are restricted in the parameter range, and it is possible that only specific classes of instabilities can be observed due to the material properties and boundary conditions of the encountered scenario *per se*.

While the postulate of the existence of cross-diffusion waves in geoscience applications is relatively new (Hu et al., 2020) they are well documented in analogous reaction-cross-diffusion systems encountered in mathematical biology (Biktashev & Tsyganov, 2016)

hydrodynamics (Schimpf & Semenov, 2004) and photonics (Paschotta, 2008). In our study they constitute the most elementary solution for low reaction rates (please refer to the parametric study in the Supporting Information). The low rates unfortunately also imply low amplitudes and low speeds of propagation. This poses challenges to how they can be detected by geological applications - are they possibly detectable with the existing methods, e.g. high sensitive pressure sensors such as pressure sensitive paints, distributed fibre-optics sensors, digital image correlation of particle image velocimetry, fibre Bragg gratings for temperature, strain gauges or acoustic emission sensors. In parallel, the premise of proposing a plausible detection system for cross-diffusion waves lies in a sound understanding of how cross-diffusion waves can manifest themselves in hydromechanically coupled problems and what we can expect in terms of detectable amplitude, spectral content and wave velocity.

In our formulation quasi-soliton (cross-diffusion) waves are a coupled set of solid and fluid pressure waves that are expected to propagate as an ensemble of self-excitation waves prior to the failure of the material. We noted earlier that they exhibit complicated wave patterns which may be difficult to distinguish from noise, partially also due to their low amplitude. In our particular formulation an instantaneous overpressure in the solid matrix generates an excess fluid pressure in the pore space which in turn promotes self-excitation of the following solid overpressure pulse triggering the next cycle. While a direct detection of both solid and fluid pressure waves is challenging in the field owing to the complex system constraints as well as the low amplitude and the complicated wave packet solutions, we found encouraging laboratory evidence on the integrated effect in recent literature. Macroscopically, the waves discussed here are dissipative P- waves which are expected to appear as propagating compaction bands. Observation of propagating compaction bands in porous media has been recorded in controlled laboratory experiments of crushed snow (Barraclough et al., 2017) and compression of puffed rice (Guillard et al., 2015). Controlled laboratory compression experiments of natural limestones have also been performed in our laboratory but convincing experimental proof is still outstanding, perhaps due to the fact that propagating cross-diffusional waves are close to the detection limit of the particle image velocimetry (PIV) apparatus.

The problem of detection of low amplitudes of cross-diffusion waves may, however, be overcome when pushing to an extreme scenario, i.e. setting the self-diffusion coefficients to zero and only considering the coupled reaction-cross-diffusion equations. For instance, the fluid and solid pressure cross-diffusion coefficients are assumed to be of opposite sign and set to unity for simplicity. For these coefficients and a specific set of reaction terms as illustrated in Regenauer-Lieb et al. (2021a) our formulation simplifies to the 1-D nonlinear Schrödinger equation. This equation has a fundamental soliton solution which in its lowest mode is known as the Peregrine soliton (Peregrine, 1983). The Peregrine soliton features a peculiar space-time focusing of wave energy such that during its peak the soliton amplifies to nearly an order of magnitude higher intensity (see Fig. 3).

A particular exciting avenue of testing the cross-diffusion wave hypothesis in geology and geophysics applications is therefore offered by trying to tackle the long-standing problem of extending empirical laboratory-based constitutive laws (e.g. rate-and-state variable friction) by insights from fundamental physics-based processes. Dynamic coefficients for the modeling of earthquake source instabilities (Tse & Rice, 1986) could e.g. be derived from a reaction-cross-diffusion formulation. This could be progressed both by controlled laboratory experiments and seismological analysis such as the interpretation of slow self-focusing Peregrine soliton-like signals prior to an earthquake. The infra- to sonic frequency gravity-seismic soliton wave (KaY-wave) that has been recorded to move toward the epicenter of a future earthquake (Koronovsky et al., 2019) may be a suitable candidate for analysis. For this investigation it is necessary to consider the complete elasto-dynamic variant (Regenauer-Lieb et al., 2021b) of the equations proposed

here. We have been able to show only that the newly discovered quasi-soliton (cross-diffusion) waves can under certain circumstances deliver a high intensity fluid pressure pulse which may be considered the physical trigger for earthquake instabilities, which suggests that exploring the elastodynamic variant should be a theme of future work.

## 5 Conclusions

In this contribution, we derived a multiphysics and multiscale approach to localisation phenomena in geomaterials by considering explicitly the feedbacks between multiple reaction-diffusion dynamic regimes regularized by considering nonlocal effect of cross-diffusional coupling. This analysis has enriched the classes of stress waves in solids (Kolsky, 1964) by three well defined domains of instability: (1) a narrow domain of Turing instabilities, (2) a broader Hopf domain instability and (3) a new domain of cross-diffusion waves. Both Turing and Hopf instabilities are here proposed to cause geological localisation structures of either brittle or ductile nature. We identified diagnostic signatures of these waves, which may be used to test their existence in nature. Turing instabilities have a characteristic wavelength $\lambda = 2\pi/k_c$, Hopf-waves show a characteristic frequency $f = 1/T = \sqrt{\tilde{a}_{11}\tilde{a}_{22} - \tilde{a}_{12}\tilde{a}_{21}}/2\pi$, and cross-diffusional quasisolitons have a characteristic FKPP wave velocity which is a material constant (Tsyganov et al., 2007).

In this work, we substantiated the hypothesis that slow waves propagating as dissipative stress/strain perturbations are a common feature in solids as a result of hierarchically organised multiscale system dynamics (Makarov & Peryshkin, 2017). Seismogenic instabilities themselves are required to couple across the entire range of length scales, from crystal-lattice (chemical) to plate-tectonic scale. This long range multiscale coupling has been proposed (Regenauer-Lieb et al., 2021b) to be facilitated by cross-diffusion waves because of their multiscale frequency spectrum. Future work invites the development of new diagnostic geological and geophysical tools to detect these new types of slow stress waves in solids.

## Supplementary material list:

(1) a linear stability analysis, (2) parametric space analysis, and supplementary movies.

Movie S1 = Turing Instability;

Movie S2 = Hopf Bifurcation;

Movie S3 = Quasi-Soliton.

**Acknowledgments**

This work was supported by: Research Grant Council of Hong Kong (ECS 27203720) and Australian Research Council (ARC DP170104550, DP170104557, LP170100233).

**Data Availability Statement:** The Finite Difference Method and simulation data can be downloaded from Mendeley Data, http://dx.doi.org/10.17632/9mkcsbk78x.1.

## References

Adomian, G. (1995). Fisher-kolmogorov equation [Journal Article]. *Applied Mathematics Letters*, *8*(2), 51-52.

Alevizos, S., Poulet, T., Sari, M., Lesueur, M., Regenauer-Lieb, K., & Veveakis, M. (2017). A framework for fracture network formation in overpressurised impermeable shale: Deformability versus diagenesis [Journal Article]. *Rock Mechanics and Rock Engineering*, *50*(3), 689-703.

Amdreo-Valle, F., Mazon, J., Rossi, D., & Toledo-Molero, J. (2010). *Nonlocal diffusion processes* (Vol. 165) [Book]. Providence, Rhode Island: American Mathematical Society.

Aydin, A., & Johnson, A. M. (1978). Development of faults as zones of deformation bands and as slip surfaces in sandstone. *pure and applied geophysics*, *116*(4), 931–942.

Ball, P. (2012). Pattern formation in nature: Physical constraints and self-organising characteristics [Journal Article]. *Architectural Design*, *82*(2), 22-27.

Barraclough, T. W., Blackford, J. R., Liebenstein, S., Sandfeld, S., Stratford, T. J., Weinländer, G., & Zaiser, M. (2017). Propagating compaction bands in confined compression of snow [Journal Article]. *Nature Physics*, *13*(3), 272-275.

Biktashev, V. N., & Tsyganov, M. A. (2016). Quasisolitons in self-diffusive excitable systems, or why asymmetric diffusivity obeys the second law [Journal Article]. *Scientific Reports*, *6*, 30879.

Bouin, E., Henderson, C., & Ryzhik, L. (2017). Super-linear spreading in local and non-local cane toads equations [Journal Article]. *Journal de Mathématiques Pures et Appliquées*, *108*(5), 724-750.

Dewers, T., & Ortoleva, P. (1990). Geochemical self-organization iii, a mechanochemical model of metamorphic differentiation [Journal Article]. *American Journal of Science*, *290*(5), 473-521.

Duszek-Perzyna, M., & Perzyna, P. (1996). Adiabatic shear band localization of inelastic single crystals in symmetric double-slip process [Journal Article]. *Archive of Applied Mechanics*, *66*, 369-384.

Eberhard, M., Savojardo, A., Maruta, A., & Römer, R. A. (2017, Oct). Rogue wave generation by inelastic quasi-soliton collisions in optical fibres. *Optics Express*, *25*(23), 28086.

Elphick, K. E., Sloss, C. R., Regenauer-Lieb, K., & Schrank, C. E. (2021). Distribution, microphysical properties, and tectonic controls of deformation bands in the miocene subduction wedge (whakataki formation) of the hikurangi subduction zone [Journal Article]. *Solid Earth*, *12*(1), 141-170.

Fisher, R. A. (1937). The wave of advance of advantageous genes [Journal Article]. *Annals of Eugenics*, *7*(4), 355-369.

Guillard, F., Golshan, P., Shen, L., Valdes, J. R., & Einav, I. (2015). Dynamic patterns of compaction in brittle porous media [Journal Article]. *Nature Physics*, *11*, 835-838.

Hobbs, B., & Ord, A. (2015). *Structural geology: The mechanics of deforming metamorphic rocks*. Oxford: Elsevier.

Hobbs, B., Ord, A., & Regenauer-Lieb, K. (2011). The thermodynamics of deformed metamorphic rocks: A review [Journal Article]. *Journal of Structural Geology*, *33*(5), 758-818.

Hu, M., Schrank, C., & Regenauer-Lieb, K. (2020). Cross-diffusion waves in hydro-poro-mechanics [Journal Article]. *Journal of the Mechanics and Physics of Solids*.

Kolmogorov, A., Petrovsky, I., & Piskunov, N. (1937). Etude de l'equation de la diffusion avec croissance de la quantite de matiere et son application a un probleme biologique [Journal Article]. *Bulletin Universite de Etat a Moscow*, *1*(1), 1-26.

Kolsky, H. (1964). Stress waves in solids [Journal Article]. *Journal of Sound and Vibration*, *1*(1), 88-110.

Koronovsky, N. V., Zakharov, V. S., & Naimark, A. A. (2019). Short-term earthquake prediction: Reality, research promise, or a phantom project? [Journal Article]. *Moscow University Geology Bulletin*, *74*(4), 333-341.

L'Heureux, I. (2013). Self-organized rhythmic patterns in geochemical systems [Journal Article]. *Philosophical Transactions of the Royal Society A: Mathematical, Physical and Engineering Sciences*, *371*(2004), 20120356.

L'Heureux, I. (2018). Diagenetic self-organization and stochastic resonance in a model of limestone-marl sequences [Journal Article]. *Geofluids*, *2018*, 4968315.

Lioubashevski, O., Arbell, H., & Fineberg, J. (1996, May). Dissipative solitary states in driven surface waves. *Phys. Rev. Lett.*, *76*, 3959–3962.

Luther, R. (1987). Propagation of chemical reactions in space [Journal Article]. *Journal of Chemical Education*, *64*(9), 740.

Makarov, P. V., & Peryshkin, A. Y. (2017). Slow motions as inelastic strain autowaves in ductile and brittle media [Journal Article]. *Physical Mesomechanics*, *20*(2), 209-221.

Ortoleva, P. J. (1993). Self-organization and nonlinear dynamics in sedimentary basins [Journal Article]. *Philosophical Transactions of the Royal Society of London Series a-Mathematical Physical and Engineering Sciences*, *344*(1670), 171-179.

Ortoleva, P. J. (1994). *Geochemical self-organization* [Book]. New,York: Oxford University Press.

Paschotta, R. (2008). Quasi-soliton pulses [Book Section]. In *Encyclopedia of laser physics and technology,* (1st edition October 2008 ed.). Wiley-VCH.

Peregrine, D. H. (1983). Water waves, nonlinear schrödinger equations and their solutions [Journal Article]. *The Journal of the Australian Mathematical Society. Series B. Applied Mathematics*, *25*(1), 16-43.

Regenauer-Lieb, K., Hu, M., Schrank, C., Chen, X., Pena Clavijo, S., Kelka, U., ... Scyzmak, P. (2021a). Cross-diffusion waves as a trigger for multiscale, multi-physics instabilities: Applications to earthquakes [Journal Article]. *Solid Earth*, *submitted*.

Regenauer-Lieb, K., Hu, M., Schrank, C., Chen, X., Pena Clavijo, S., Kelka, U., ... Jacquey, A. (2021b). Cross-diffusion waves as a trigger for multiscale, multi-physics instabilities: Theory [Journal Article]. *Solid Earth*, *12*, 869–883.

Regenauer-Lieb, K., Veveakis, M., Poulet, T., Wellmann, F., Karrech, A., Liu, J., ... Fusseis, F. (2013). Multiscale coupling and multiphysics approaches in earth sciences: Applications [Journal Article]. *Journal of Coupled Systems and Multiscale Dynamics*, *1*(3), 2330-152X/2013/001/042.

Schimpf, M. E., & Semenov, S. N. (2004). Symmetric diffusion equations, barodiffusion, and cross-diffusion in concentrated liquid mixtures [Journal Article]. *Physical Review E*, *70*(3), 031202.

Tse, S. T., & Rice, J. R. (1986). Crustal earthquake instability in relation to the depth variation of frictional slip properties [Journal Article]. *Journal of Geophysical Research-Solid Earth and Planets*, *91*(B9), 9452-9472.

Tsyganov, M. A., & Biktashev, V. N. (2014, Dec). Classification of wave regimes in excitable systems with linear cross diffusion. *Phys. Rev. E*, *90*, 062912.

Tsyganov, M. A., Biktashev, V. N., Brindley, J., Holden, A. V., & Genrikh, R. I. (2007). Waves in systems with cross-diffusion as a new class of nonlinear waves [Journal Article]. *Physics-Uspekhi*, *50*(3), 263.

Vanag, V. K., & Epstein, I. R. (2009). Cross-diffusion and pattern formation in reaction–diffusion systems [Journal Article]. *Physical Chemistry Chemical Physics*, *11*(6), 897-912.

Vardoulakis, I., & Sulem, J. (1995). *Bifurcation analysis in geomechanics* [Book]. Glasgow: Blankie Acc. and Professional.

Veveakis, E., & Regenauer-Lieb, K. (2015). Cnoidal waves in solids. *Journal of the Mechanics and Physics of Solids*, *78*, 231-248.

Volpert, V., & Petrovskii, S. (2009). Reaction–diffusion waves in biology [Journal Article]. *Physics of Life Reviews*, *6*(4), 267-310.

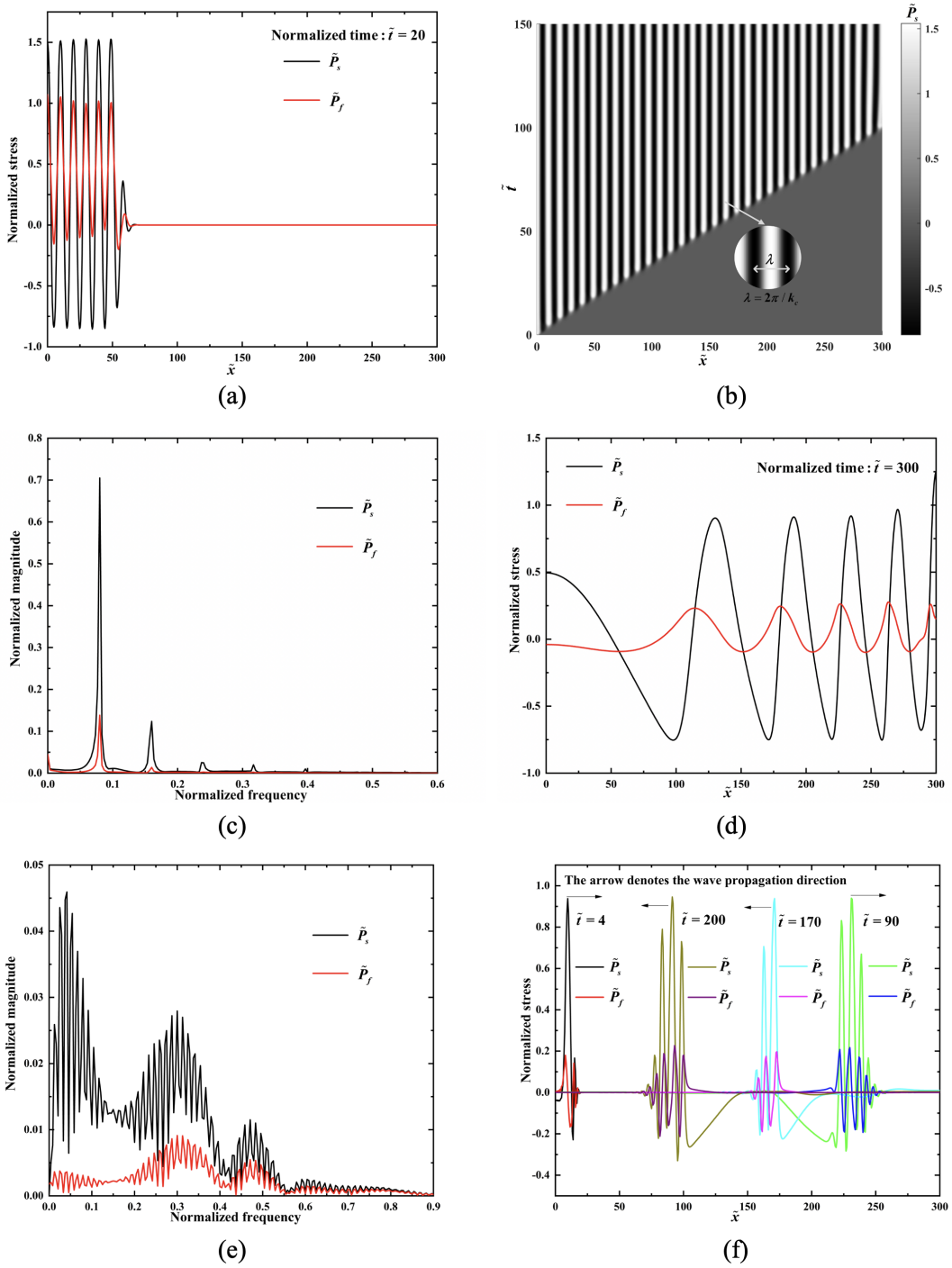


**Figure 1.** Three types of instabilities. Type-I bifurcation (Turing instability): a) propagating standing wave before reaching the boundary; b) final standing-wave pattern. The dimensionless group of parameters used: $\tilde{a}_{11} = 1.5, \tilde{a}_{12} = -1.3, \tilde{a}_{13} = 1, \tilde{a}_{14} = -1, \tilde{a}_{21} = 2, \tilde{a}_{22} = -1.6, \tilde{D}_M = 1, \tilde{D}_H = 3, \tilde{d}_M = 2, \tilde{d}_H = -1.5$. Type-II (Hopf) bifurcation: c) Hopf waves in frequency domain; d) travelling Hopf waves in space domain. The dimensionless group of parameters used: $\tilde{a}_{11} = 0.3, \tilde{a}_{12} = -3, \tilde{a}_{13} = 0.5, \tilde{a}_{14} = -0.5, \tilde{a}_{21} = 0.1, \tilde{a}_{22} = -0.1, \tilde{D}_M = 0.1, \tilde{D}_H = 0.1, \tilde{d}_M = -1, \tilde{d}_H = 1$. Type-III bifurcation (Quasi-soliton wave): e) Quasi-soliton waves in frequency domain; f) travelling Quasi-soliton waves before and after reflection in space domain. The dimensionless group of parameters used: $\tilde{a}_{11} = -0.05, \tilde{a}_{12} = -3, \tilde{a}_{13} = 1, \tilde{a}_{14} = -1, \tilde{a}_{21} = 0.01, \tilde{a}_{22} = 0, \tilde{D}_M = 0.01, \tilde{D}_H = 0.01, \tilde{d}_M = -1, \tilde{d}_H = 1$.

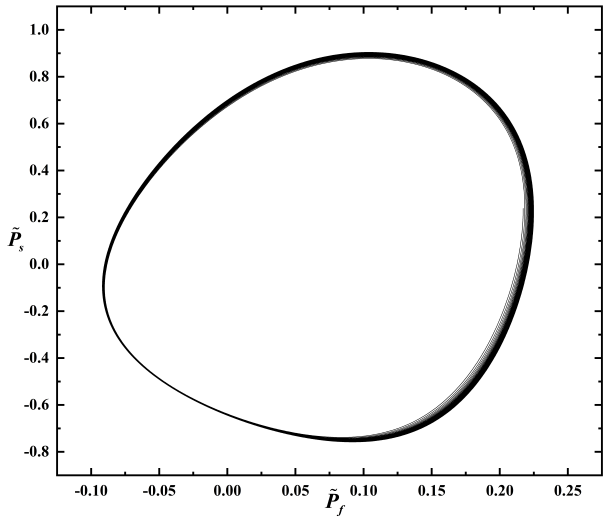


**Figure 2.** Phase diagram of Hopf bifurcation upon reaching stable orbits (clockwise oscillation).

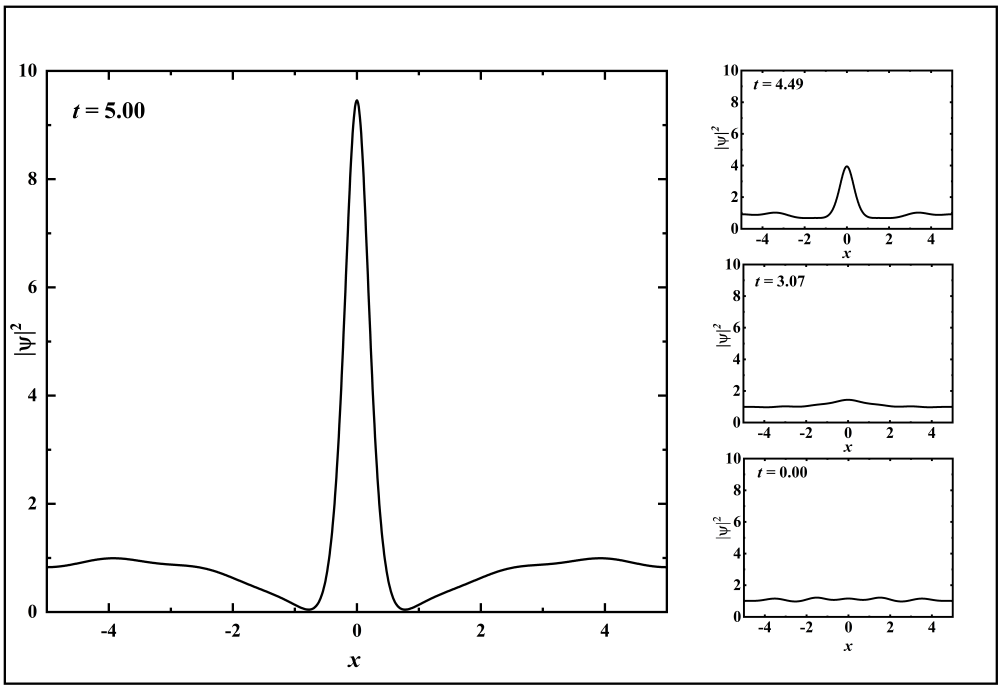


**Figure 3.** The Peregrine soliton compresses wave energy from the environment into a singular rogue wave event. Note that just before the emergence of the soliton at x=0 and t=3.07 (middle right panel) the background oscillations are smoothed.